Macromolecules

ARTICLE

pubs.acs.org/Macromolecules

Shape-Dependent Localization of Carbon Nanotubes and Carbon Black in an Immiscible Polymer Blend during Melt Mixing

Andreas Göldel,[†] Abraham Marmur,[‡] Gaurav R. Kasaliwal,[†] Petra Pötschke,*[,†] and Gert Heinrich[†,§]

[†]Leibniz Institute of Polymer Research Dresden, Hohe Str. 6, 01069 Dresden, Germany

[‡]Chemical Engineering Department, Technion - Israel Institute of Technology, Haifa 32000, Israel

[§]Institute for Materials Science, Technische Universität Dresden, Helmholtzstrasse 7, 01069 Dresden, Germany

ABSTRACT: In melt mixed multiphase polymer blends, the mechanisms determining the spatial distribution and localization of solid particles smaller than the blend domain sizes are still not completely understood. From theoretical considerations of a previous paper of one of the authors, it was derived that the transfer dynamics as well as the stability of different solid fillers at the blend interface reveal a strong dependence on the particle's aspect ratio. Low interfacial stabilities and high transfer speeds between the blend phases can be deduced for fillers with very high aspect ratios, entitled as the "Slim-Fast Mechanism" (SFM). The SFM appears suitable to explain in retrospect important features of several previous studies that address the localization of differently shaped nanoscaled particles in polymer blends. The SFM was evaluated by investigating the simultaneous transfer of multiwalled carbon nanotubes (MWCNTs) and carbon black (CB) from a poly(styrene acrylonitrile) (SAN) precompound into the thermodynamically preferred initially unfilled polycarbonate (PC) phase during melt mixing.

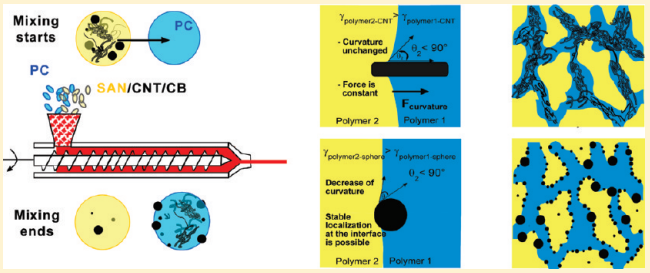

1. INTRODUCTION

Compared to single-polymer composites, the combination of multiphase polymer blends with conductive nanoscaled fillers offers a much higher potential for the development of conductive composites with very low filler concentrations. Among the various combinations of filler localizations and phase structures that can be formed in phase-separated blend systems, those structures are especially promising where the fillers are either selectively localized in one of the blend phases or at the interface of an immiscible cocontinuous blend. Such morphologies can potentially result in low and ultralow electrical percolation thresholds.[1,2] Thus, understanding and control of the localization phenomena of solid nanofillers in polymer blends are the keys toward new tailor-made materials.

Whereas localization of the filler at the interface is expected to be the ideal scenario to reach the lowest possible electrical percolation concentration, this structure has so far been observed only once for melt mixed blends with carbon nanotubes (CNTs).[3,4] In contrast, blends with selectively CNT filled phases can already today be prepared by melt mixing,[5−14] thus enabling the manufacturing of double percolated structures.[6−8,10−14] The term double percolation describes the percolation of a selectively filled blend phase in combination with a percolated network of fillers within this phase that enables the formation of conductive pathways through the whole sample. This concept was first described in 1991 for blends with carbon black (CB).[1]

In contrast to the comprehensive experience with CB, concentrated efforts to manufacture conductive thermoplastic polymer blends with multiwalled carbon nanotubes (MWCNTs) by melt processing did not start until the year 2002. The results that were published since then indicate that for MWCNTs the distinctive selective and exclusive localization in one of the blend phases is very likely after melt mixing.[5−14]

Different concepts are described in literature to explain the localization of solid nanofillers in polymer blends. Some authors attributed the observed particle arrangements to melt viscosity effects,[15−17] but most frequently nanofiller localization is explained by the system's tendency to minimize its free energy. One possibility to express this generally valid principle is the wetting coefficient ω_a^1 that is derived from the Young's equation.[18] Examples can be found for blends with nanosilica,[19−21] carbon black,[1,17,22] and CNTs.[4,6−8,23,24]

Unfortunately, the different approaches can presently not be summarized to a consistent concept that is able to explain and predict the localization of CNTs in so far not investigated blend systems.[20,25] The insufficient knowledge about the surface properties of CNTs and their interactions with macromolecules is one of the main inhibiting factors in this context.

To the best of our knowledge, the geometry of nanoparticles has so far never been considered as a significant parameter for the filler localization within the blend morphology. On the basis of the considerations of a purely theoretical paper,[26] a strong aspect ratio dependence was concluded for the localization behavior of nanoparticles. The derived dependency affects both

Received: April 5, 2011
Revised: June 10, 2011
Published: July 13, 2011

the thermodynamically most stable localization in the blend and the speed of a possible nanofiller transfer between two blend phases. In this study, the validity of the proposed correlations is evaluated based on several previous studies and for different nanoparticles.

Furthermore, the aspect ratio dependency is experimentally verified by the investigation of the simultaneous transfer of MWCNTs and CB from a poly(styrene acrylonitrile) (SAN) precompound into an initial unfilled polycarbonate (PC) phase. The selected PC/SAN blend serves as a model system for the commercially important PC/acrylonitrile−butadiene−styrene (ABS) blends.

2. EXPERIMENTAL SECTION

2.1. Materials. Bisphenol-A-based polycarbonate Makrolon 2600 and MWCNTs Baytubes C150HP were supplied by Bayer MaterialScience AG (Leverkusen, Germany). According to the supplier, the employed high purity (HP) grade of MWCNTs has outer diameters from 13 to 16 nm and a carbon purity of more than 99%.[27] According to ref 28, 90% of the pristine MWCNTs are shorter than 1.7 μm. Styrene−acrylonitrile statistical copolymer Luran 358N was received from ALBIS Plastic GmbH. The molar fraction of the acrylonitrile (AN) group of SAN dissolved in dichloromethane was determined via liquid NMR measurement to be 23 ± 1 wt %, corresponding to 37 ± 1 mol %. NMR spectra were recorded on a DRX 500 spectrometer (Bruker, Germany) operating at 500.13 MHz for ^{1}H and 125.75 MHz for ^{13}C. There is evidence that at AN contents around 25 wt % the optimum thermodynamic interaction in between PC and SAN copolymers can be observed.[29] The zero shear viscosities as measured using an oscillatory ARES rheometer (TA Instruments, formerly Rheometric Scientific) at 260 °C were 1.7×10^3 and 9.8×10^2 Pa·s for Makrolon 2600 and Luran 358, respectively. At 100 rad s^{-1}, the viscosities dropped to 1.2×10^3 Pa·s for PC and 4.0×10^2 Pa·s for SAN.

For the preparation of PC/SAN blends with CB and CNTs, a low structured carbon black, namely Printex 35 (labeled "CB") from Evonik AG (Marl), was employed.

2.2. Mixing Procedures. A discontinuous DSM Xplore 15 mL twin-screw microcompounder (referred as DSM 15) was employed for the melt blending. The compounder includes a bypass that enables a circulating melt flow from the corotating conical screw ends to the feeding zone and therefore allows the independent variation of mixing time and screw speed. To enable the comparison of experimental results with previous investigations,[6] the processing conditions were selected accordingly. For the first set of experiments, 1 wt % CB and 1 wt % MWCNTs were predispersed in SAN for 5 min at 280 °C barrel temperature and a screw speed of 100 rpm. Subsequently, the SAN-matrix precompound was melt blended in a separate mixing step with PC. The blend consists of 40 wt % of the SAN-CNT-CB precompound and 60 wt % of neat PC. In a second set, 1 wt % CB, 1 wt % MWCNTs, 40 wt % SAN, and 60 wt % PC were mixed simultaneously by applying the same processing conditions as for the first set.

2.3. Microscopy. Transmission electron microscope (TEM) investigations were performed on unstained ultrathin sections of approximately 80−100 nm thickness using a Zeiss Libra 200 microscope operated at 200 kV. The sections taken from the center of the extruded strands were prepared at room temperature.

3. THEORETICAL BASIS

3.1. Nanofiller Localization in Immiscible Polymer Blends. Because of the short processing times, commercial manufacturing of polymer blends with solid fillers using twin-screw extrusion is determined by the interplay between thermodynamic driving forces and kinetic factors. Therefore, nonequilibrium filler localization states can be obtained, specifically if the filler is initially localized within the thermodynamically less favorable blend phase. Then, the transfer rate can determine the final localization of the filler in the blend. In the literature, the filler localization in melt mixed blends is sometimes explained with viscosity effects,[15−17] but the different results and interpretations cannot be summarized to a clear trend or concept and sometimes are even opposing each other.[16,25,30] The presently insufficient knowledge originates from the difficulties to disconnect viscosity effects from other localization relevant parameters such as thermodynamic driving forces, mixing regime, and the melting temperatures of the employed polymers. Generally, the filler's thermodynamically preferred localization in the blend phases should not be affected by the polymer viscosity that therefore should only be relevant for nonequilibrium states and thus insufficient mixing procedures. Correct interpretation of these intermediate states affords knowledge about the thermodynamic equilibrium that is theoretically obtained after infinite mixing time and practically corresponds to processing-stable nanofiller localization in the blend. The prominence of interfacial effects and thermodynamic driving forces is generally increasing with decreasing melt viscosities and increasing mixing times. The fast and complete transfer of CNTs from SAN into PC[6] reveals that nanofillers can nevertheless quickly overcome the blend interface also for high melt viscosities of both blend phases. Furthermore, the transfer in these blends occurs from the lower to the higher viscosity phase.

Summarizing the state of the art, the dominating influence of interfacial effects and thermodynamic driving forces on the localization behavior is widely accepted specifically for nanoscaled fillers. One possibility to express the thermodynamic preference is given by the wetting coefficient ω_a that was adapted by Sumita et al.[1] from Young's equation:[18]

$$\omega_a = \frac{\gamma_{\text{filler-polymer 1}} - \gamma_{\text{filler-polymer 2}}}{\gamma_{\text{polymer 1,2}}} \quad (1)$$

In this equation, the symbols γ_x denote in the numerator the different interfacial tensions between filler and polymers 1 and 2 and in the denominator the interfacial tensions between the two blend phases. The coefficient can be understood as a simple mathematical description of the thermodynamic tendency of fillers to localize in that particular position in the immiscible blend that corresponds to the minimization of the three relevant interfacial tensions. Nevertheless, it significantly suffers from the difficulties to accurately measure γ between nanoparticles and liquids. The measurement problems arise from the macro-, micro-, and nanostructure of the agglomerated nanoscaled surfaces of the filler. Thus, all standard measurement methods that are based on the contact angle or capillary effects are significantly disturbed by the surface structure, and the obtained values can strongly deviate from the real surface properties of an individual nanoparticle. Therefore, the direct measurement of the interfacial tensions between the blend polymers and macroscopic samples prepared from the respective nanofiller is not appropriate. Basically, it is possible to overcome these difficulties by the calculation of the interfacial tensions/energies from surface energy values for CNTs and blend polymers, as it is state of the art for blends with CNTs. Nevertheless, the described difficulties impede as well the determination of accurate surface energy values for CNTs that are the precondition for the calculation. The present insecurity is clearly visible when

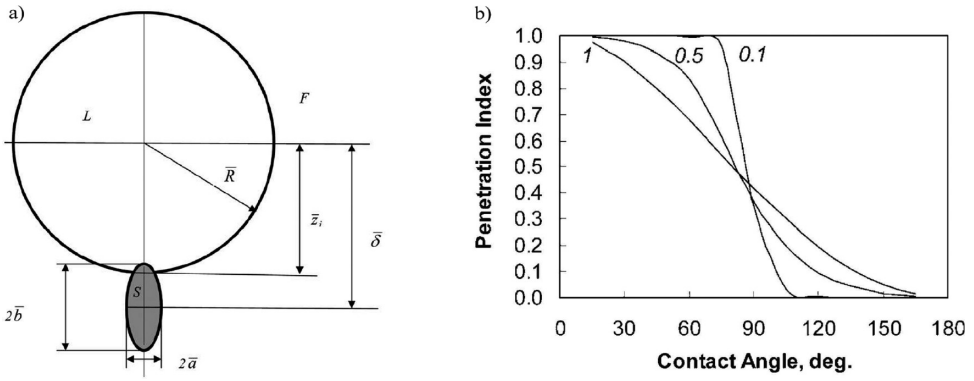

Figure 1. Solid particle at the interface of a liquid drop and a surrounding liquid:[26] (a) geometric arrangement; (b) correlation of penetration index and contact angle for different particle aspect ratios ($2a/2b$ = 1, 0.5, and 0.1), assuming negligible line tension.[26] The penetration index is defined as the percentage of the particle penetration into the drop. Reproduced with permission from ref 26. Copyright 2005 Taylor and Francis.

regarding the surface energy values for carbon nanotubes that have been published so far. Total surface energies between 28 mJ/m^2,[31] and above 114 mJ/m^2,[32] and polarity values between 0%[33] and 59%[34] can be found. Beyond the uncertainty of the measurement, the authors of studies on polymer blends with CNTs mostly do not find surface energy data for the individual CNT grade that is used in their investigation. Thus, the values are commonly freely selected from the broad spectrum of surface energies. It is obvious that the localization prediction using the wetting coefficient can strongly depend on the selected values and thus can once be consistent with the actually observed filler localization and once not. These uncertainties of the prediction are further emphasized by the strong dependence of the CNT surface properties on the production method and on subsequent surface treatments.[35]

Summarizing and despite the importance of the topic, at present it is not possible to reliably predict the localization behavior of nanofillers in a melt mixed multiphase polymer blend,[25] even if in many cases the prediction of the wetting coefficient was reported to agree with experimental findings.

Nevertheless, one tendency appears to be prevalently observable from the available literature: the transfer of nanoparticles through a blend interface appears to be fast for high aspect ratio fillers like CNTs and slower and less effective for particles with low aspect ratios such as carbon black. Thus, unfunctionalized CNTs are frequently highly selective localized within the thermodynamically preferred phase after typical mixing processes.[5−8,10−13]

In contrast, particles with low aspect ratios often are distributed in between the unfavorable (if predispersed there) and the favorable blend phase. Furthermore, their interfacial stability seems to be significantly higher than that of high aspect ratio fillers. Thus, they can be additionally, preferentially or exclusively localized at the interface of nonreactive immiscible blends. This behavior is visible for example for carbon black[1,2,36−44] or aggregated spherical silica particles[19,20] and thus for fillers with almost ideally low aspect ratios.

To the best of our knowledge, the observed localization behavior has never been connected to the geometrical shape of the incorporated particles.

3.2. Equilibrium State of Ellipsoidal Solid Particles at a Liquid−Liquid Interface. When adapting the theoretical calculations of Krasovitski and Marmur[26] toward multiphase blend systems, the observed differences in the localization behavior of different nanofillers can be explained. The authors mathematically derived the thermodynamically most stable position of ellipsoidal solid particles at liquid−liquid interfaces for the equilibrium state (Figure 1a).

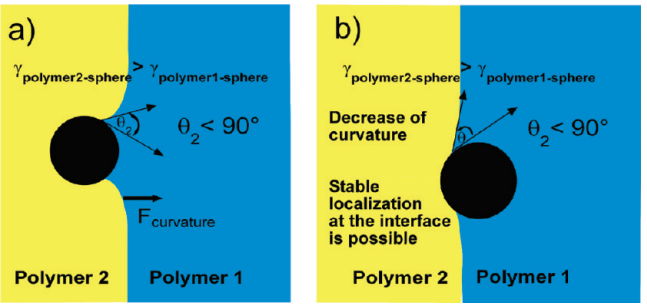

Figure 2. Ideal low aspect ratio filler (not slim) at the blend interface during melt mixing. The interfacial curvature can relax while θ_2 is constant, and thus the driving force $F_{curvature}$ is decreasing during the transfer.

The calculations show that the equilibrium position strongly depends on the particle aspect ratio. A spherical particle that is located at the interface of a drop and a surrounding liquid penetrates into both liquids for a broad range of contact angles between the particle and the liquid−liquid interface. The area part of the particle that is in the respective liquid phase (penetration index, Figure 1b) varies according to the contact angle.

In strong contrast, a particle with a high aspect ratio (e.g., $2a/2b$ = 0.1, Figure 1a,b) either penetrates into the drop completely or remains in the liquid. Complete coverage by one of the liquids is obtained even when the particle is only slightly better wetted by one of the liquids and thus almost independent of the actual value of the contact angle. Thus, an increase in the particle aspect ratio corresponds to a sharper dependence of the penetration index on the contact angle.

3.3. Transfer of Real Nanofillers through a Blend Interface: The Slim-Fast Mechanism (SFM). From the presented theoretical concept one can derive that the particle aspect ratio is also highly relevant for nonequilibrium processes such as melt blending and as well for nonellipsoidal and thus real nanoparticles. Strong influence on the interfacial stability and the transfer speed can be deduced.

Adaptations of the concept for a nanoparticle that comes close to the blend interface during melt mixing are illustrated in

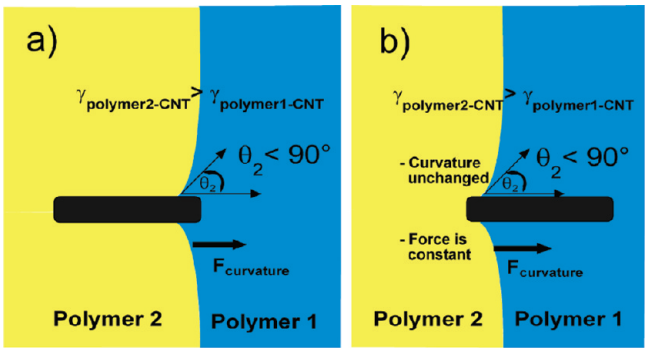

Figure 3. High aspect ratio filler (slim) at the blend interface. The interfacial curvature is not able to relax when θ_2 remains constant. Thus, the driving force is not decreasing during the transfer.

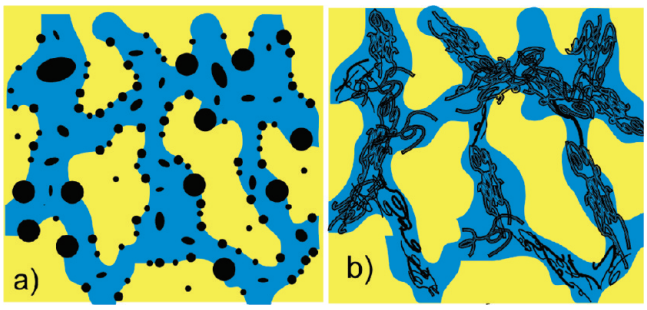

Figure 4. Typical localization scenarios for low (a) and high (b) aspect ratio fillers that were predispersed within a poor wetting blend phase (yellow) and subsequently melt-blended for same mixing times with a more favorable polymer (blue): (a) Spheres and ellipsoidal particles are distributed in between the blend interface and the preferred (blue) blend phase according to their interfacial stability. (b) Slim CNTs are highly selective localized in the preferred blend phase (blue) after melt blending.

Figures 2 and 3. Particle transfer through the blend interface occurs when the filler is initially located in the less favorable wetting blend phase (here polymer 2). When the flow field induces contact of interface and nanoparticle, the molecules of the more favorable blend phase (polymer 1) that are close to the interface will advance on the particle surface and thus, if possible, substitute those of polymer 2. This results in a thermodynamically instable curvature that is determined by the equilibrium wetting angle θ_2. In the initial state of the transfer, the curvature is on an equal level for spheres and rods (Figures 2a and 3a). To achieve a more stable configuration, the interface relaxes by decreasing the curvature to some degree, which drives the wetted particle a certain distance into the more favorable wetting phase. As this movement increases the wetting angle of the preferred phase θ_2, the molecules of this phase advance again some distance on the surface of the particle, until the equilibrium wetting angle is restored. Each of these cycles results in an increasing part of particle surface being covered by the more favorable wetting phase. To get a feeling for the real process, one has to imagine an infinite number of infinitesimal small relaxations and advances that finally transfer the particles into the phase with the more favorable particle wetting.

To understand why high aspect ratio objects are transferred faster and more efficient as compared to those with low aspect ratios, one has to consider the change of the blend interface curvature during the transfer process. Generally, the instability of the curvature is generating the driving force ($F_{curvature}$) for the transfer of the solid particle.

Figure 2a,b illustrates that the geometrical peculiarities of spherical particles enable the relaxation of the curvature by a small shift of the particle position toward the better wetting phase. Thus, particles with low aspect ratios and ellipsoidal surfaces can maximize their thermodynamic stability at the blend interface by moving in the direction of the better wetting blend phase while the equilibrium wetting angle θ_2 at the ternary interface remains unchanged.

In contrast, this is not possible for rodlike particles. The curvature of the blend interface induced by the rod is independent from its movement toward the better wetting phase. Thus, $F_{curvature}$ is not decreasing during the motion of the rod toward polymer 1. The blend interface can only relax after the rod has been completely transferred (Figure 3a,b). Therefore, its stability at the blend interface is low, provided that the long axis of the filler is orientated perpendicular or significantly off-axis to the direction of the blend interface. The transfer should thus be faster and more effective than that of a low aspect ratio particle with a similar wetting angle. This provides a reasonable explanation for the fast and complete transfer of CNTs from a less favorable into a more favorable wetting blend phase (Figure 4b) that has for example been comprehensively described for PC/SAN blends with MWCNTs.[6]

Thus, the probability of filler localization in both immiscible blend phases or at the blend interface after melt mixing is decreasing with increasing aspect ratios (Figure 4b).

We propose to address this fundamental difference as the "Slim-Fast Mechanism" (SFM), as the transfer of "slim" nanofillers (Figure 3) should occur significantly faster than that of "chubby" ones (Figure 2). This mechanism should be valid for all fillers that are sufficiently small as compared to the size of the typical features of the blend morphology.

3.4. Particle-Shape Dependent Interpretation of the Wetting Coefficient. The presented findings affect also the interpretation of the wetting coefficient. Usually ω_a is interpreted as proposed by Sumita et al.[1] Fillers are expected to be located at the interface for ω_a values in the interval between 1 and −1, whereas lower or higher values correspond to the localization in one of the blend phases. The wetting coefficient was interpreted accordingly in several publications discussing the MWCNT localization behavior in multiphase mixtures.[4,6−8,23,24] From the calculations of Krasovitski and Marmur,[26] one can derive that the interval of stable filler localization at the blend interface will strongly narrow as the effective aspect ratio of the solid filler increases.

3.5. Inhibition of the Slim-Fast Mechanism. For an individual tube, the interval narrows the less the lower the angle in between the blend interface and the filler's length axis. Thus, the probability of interface localization increases with decreasing angle. For parallel orientation, the SFM is suspended (Figure 5c,d).

Generally, the probability for interface coverage rises with increasing interfacial tension between the two polymers. By localizing at the blend interface, the filler can minimize the system's free energy by protecting the two "opposing" polymers from each other, as it has been observed for example for PP/PC blends with montmorillonite (MMT)[45] and PBT/PE blends with layered silicate.[46] There, the localization at the interface is promoted by both the only moderate aspect ratio and the significant interface coverage of each individual layer due to its two-dimensional shape. For CNTs, the effect of interfacial energy minimization is lower due to their one-dimensional shape.

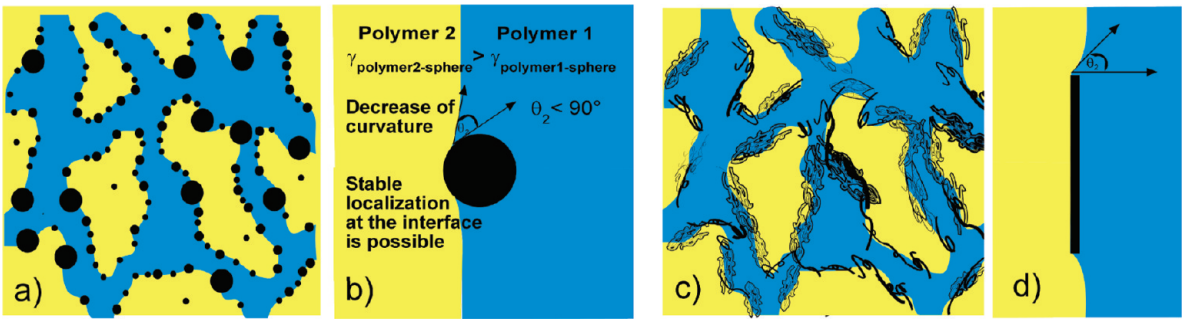

Figure 5. Low aspect ratio particles can be localized thermodynamically stable at the blend interface even if they are significantly better wetted by one of the blend phases. The most stable state is described by the penetration index (Figure 1b) that is a function of the wetting angle. In the example, the spheres (a) penetrate to a bigger part into the better wetting (blue) blend phase, thus approaching their equilibrium position at the blend interface (b). (c, d) Probability of thermodynamic stable localization at the blend interface of slim fillers increases with decreasing angle between blend interface and filler length axis. In case of parallel orientation (c,d), the biggest part of the tube length retards the transfer. Thus, the highest possible interfacial stability is obtained.

Beyond these geometrical considerations, there are some other phenomena that can disrupt the SFM. First, fillers that have been chemically coupled to one of the blend phases before or during blending cannot be transferred by the SFM. Second, the irreversible physical adsorption of one polymer phase on the surface of high aspect ratio fillers such as CNTs can also suspend the SFM. The stable localization of a significant amount of high aspect ratio MWCNTs at a blend interface has so far been observed only once for polyamide/ethylene acrylate copolymer blend systems with industrial nanotubes and was attributed to such adsorption phenomena.[3,4]

The impact of irreversible adsorption or chemical coupling on the CNT localization during melt mixing would most likely be the same. If present, the sections of the tube where polymer chains are either adsorbed or coupled can possibly be anchored in the less favorable blend phase, while the free end of the tube still experiences a thermodynamic driving force into the more favorable wetting phase. For the described PC/SAN model blends[6] and even for CNT predispersion in SAN, a simultaneous interfacial contact of CNTs with both blend phases can only be found as an exception or by intensive search in TEM investigations. Thus, this study's results as well as that of several other studies dealing with the localization of all kinds of nanoscaled fillers including CNTs reveal features that can be explained with the SFM.

3.6. Aspect Ratio of Nonideal Nanoscaled Fillers. Nevertheless, for real fillers it is always important to check whether the theoretically assumed aspect ratios reflect the real particle shapes in the polymer melt. Specifically for CNTs the actual aspect ratio is strongly dependent on the dispersion state. Only individual and stiff CNTs reveal high effective aspect ratios. Agglomerates or curved and coiled shapes of individual MWCNTs that can be frequently found when melt-processing commercial grades correspond to significantly lower aspect ratios (Figure 6). Thus, for the transfer speed, a differentiated view on the spectrum of actual nanotube shapes during melt mixing is required.

During the melt-blending process, the transfer of CNTs will be fast when the parts of the nanotubes belonging to section 2, Figure 6 (exception from SFM), and section 3 (low aspect ratio) are small as compared to section 1. Then, the transfer is dominated by the accelerating section 1 and occurs according to the SFM. Therefore, after a standard melt mixing process, there should be only very few CNTs bridging both phases as this corresponds to the highest driving forces and the lowest

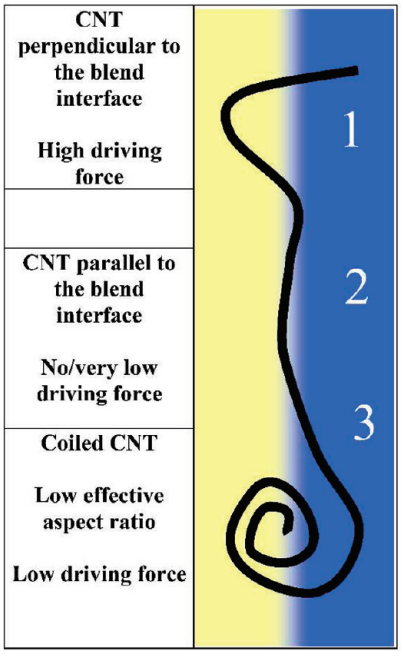

Figure 6. Shape of typical commercial MWCNTs and the shape-dependent efficiency of the SFM. Sections that accelerate the transfer (section 1) have to be distinguished from slow-down sections (sections 2 and 3).

interfacial stability. The probability of processing-stable localization of an individual CNT at the blend interface is increasing with the percentage of retarding sections within the tube. Thus, the transfer speed also depends on the orientation of the CNTs in the moment where mixing induces the first contact with the blend interface. In strong contrast to CNTs, CB reveals low aspect ratios regardless of its dispersion state. For these fillers, the differentiation between different dispersion states is not as important as for CNTs.

In the results part, the fundamental difference of interfacial stability and transfer speed for fillers with different aspect ratios that was derived from the SFM is experimentally verified.

4. RESULTS AND DISCUSSION

4.1. MWCNTS in PC/SAN Blends. In a previous work,[6] we have shown that after 5 min melt mixing of PC and SAN the

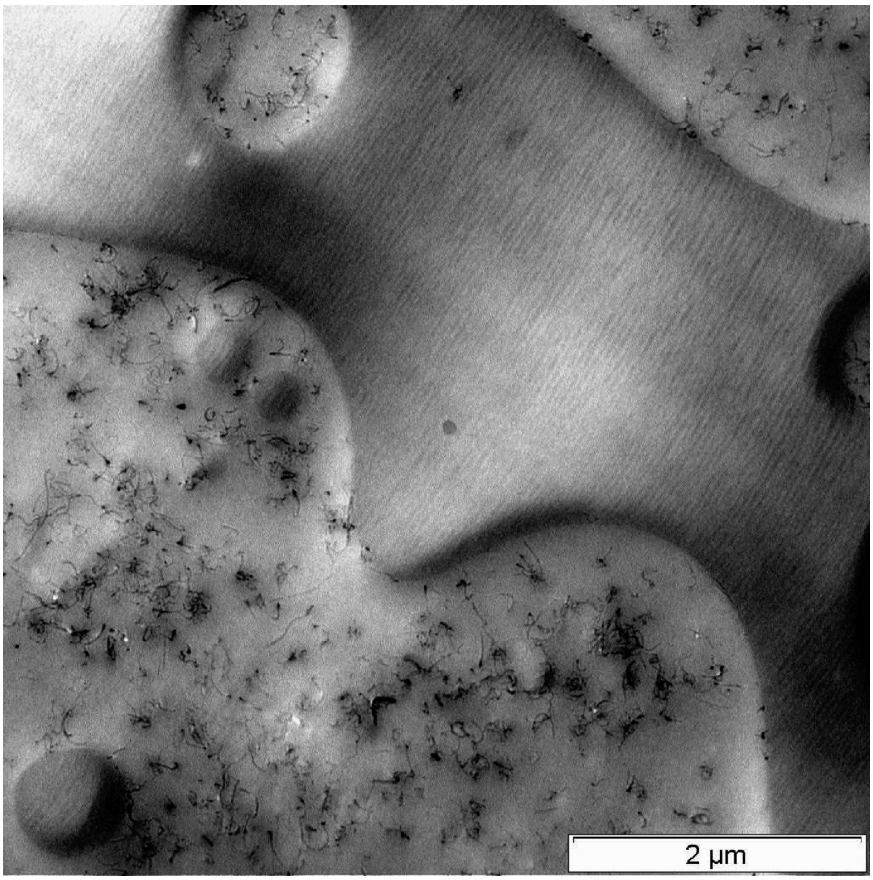

Figure 7. TEM micrograph of a PC/SAN blend with 2 wt % MWCNT in the PC phase, melt-blended for 5 min at 280 °C barrel temperature and 100 rpm in a microcompounder.[6]

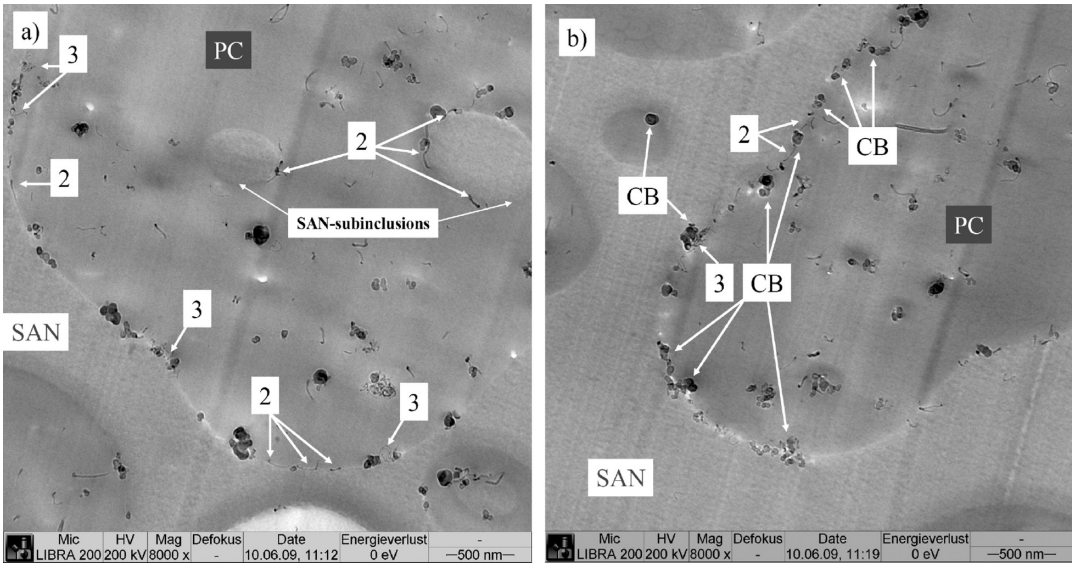

Figure 8. Localization of MWCNTs and CB in cocontinuous blends of PC and SAN (PC_{60}/SAN_{40}). The blend was prepared by predispersing CB and CNT in SAN and then blending with PC. The SAN phase appears little brighter than the PC phase and shows some characteristic roughness. CNTs located at the interface can be assigned to the exceptions from the Slim-Fast Mechanism (sections 2 and 3 in Figure 6, here labeled as "2" and "3"). To avoid excessive masking of the image, CB was labeled only in (b), whereas (a) focuses on the localization of CNTs.

incorporated MWCNTs are always exclusively located within the PC phase of the blend, independent of the applied mixing regime (Figure 7). The CNTs were even then found to be completely localized within the PC phase when they were predispersed in SAN before subsequent melt blending with neat PC. The CNT transfer from SAN to PC during melt mixing

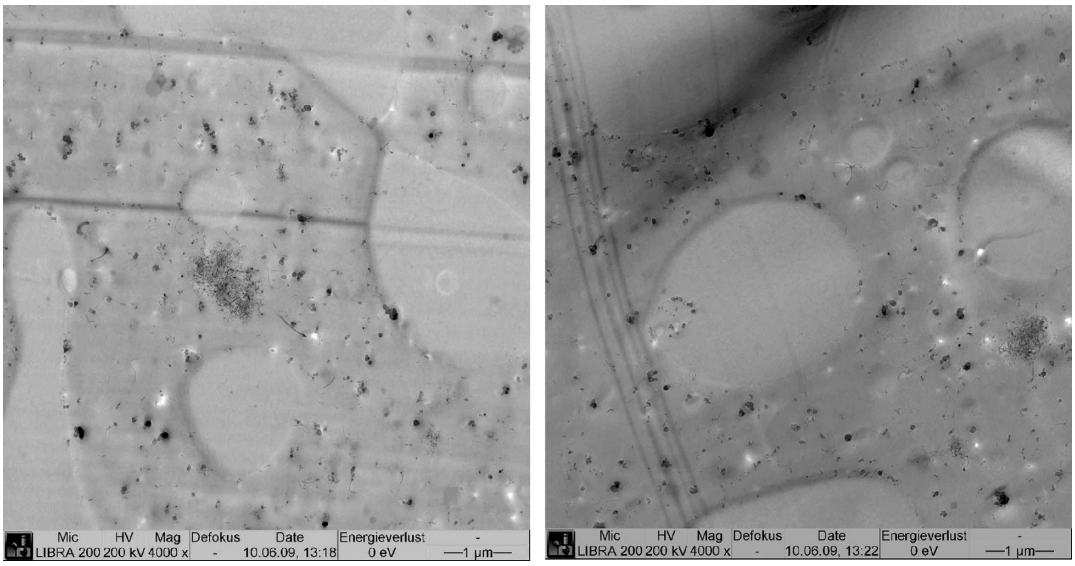

Figure 9. Localization of MWCNTs and CB in a cocontinuous PC_{60}/SAN_{40} blend prepared by one-step mixing of all four components (SAN phase: bright; PC-phase: gray).

Table 1. Classification of the Transfer Speed and Interfacial Stability of Small Objects in Polymer Blends during Melt Mixing

The Slim Fast Mechanism (SFM)						
Group I: Low aspect ratio objects – slow transfer – high interfacial stability						
Class	**CNT**	**CNT**	**CB**	**CB**	**CB**	**MMT/ Clay/ Graphite**
Scale	Macro- micro	Micro	Meso-micro	Micro-nano	Nano	Micro
Description	Primary agglomerate	Coiled CNT	Agglomerate	Aggregate	Nano-Aggregate	Stack
Scheme						
Intermediate transfer speeds/interfacial stabilities		**Group II: High aspect ratio nano objects – fast transfer-low interfacial stability**				
Class	**MMT/Graphene/ Silica**	**CNT**	**CNF**	**Halloysite**	**Other Nanotubes and -fibers**	
Scale	Nano in 1 dimension	Nano in 2 dimensions	Nano in 2 dimensions	Nano in 2 dimensions	Nano in 2 dimensions	
Description	Exfoliated or single sheet	Separated, linear CNT	Separated, linear CNF	Separated, linear tube	Separated, linear tube	
Scheme						

has, beyond our first investigations on this topic, been verified by several additional methods, including EDS/SEM (energy dispersive X-ray spectroscopy in scanning electron microscope) and EFTEM (energy-filtered transmission electron microscope) analysis.

Corresponding to the predictions that can be derived from the above-mentioned theoretical concept, separated tubes are rarely found at the interface of these blends. If they are at the interface, they are mostly coiled or connected to other coiled tubes forming microagglomerates or dominated by the parts corresponding to section 2 in Figure 6. Therefore, the localization behavior of Baytubes C150HP in the investigated PC/SAN blends is consistent with the principles of the SFM.

4.2. Simultaneous Transfer of Carbon Black and MWCNTS through the Blend Interface. In order to evaluate the validity of the concept beyond the described experimental results and the discussed literature, we aimed at investigating a system where two fillers with strongly differing aspect ratios are simultaneously transferred between the blend phases. Therefore, a blend system would be highly desirable, where both fillers are initially localized

in the same blend phase and where both fillers reveal a comparable higher affinity toward the initially unfilled blend phase. Thus, from the share of particles transferred to the more favorable phase and the share that is localized at the interface after blending, one could derive conclusions for the interfacial stability and speed of particle transfer. Carbon black appears to be the ideal counter partner for MWCNTs, as it also reveals a carbon-based surface while the aspect ratio is in all possible dispersion states very low.

For (PC/SAN)−MWCNT blends the transfer of MWCNTs from SAN toward the PC phase has been shown in our previous works.[6] For CB, the thermodynamic preference in the PC/SAN model blend was unknown. Aiming at a simultaneous transfer of CB and MWCNTs from one phase to the other, CB and MWCNTs were first predispersed within the SAN phase. This precompound was subsequently blended in a second step with the neat polycarbonate.

Figure 8 shows TEM images of the final blend morphology that was obtained after 5 min melt blending. The phases were assigned to PC and SAN via EFTEM (energy-filtered TEM) investigations relying on the characteristic elements nitrogen within SAN and oxygen within PC that are not contained in the respective other phase. As expected and in accordance with our previous investigations, the predominant fraction of CNTs migrated from SAN into PC.

The MWCNTs that are located at the interface are either oriented parallel to the interface (Figure 6, "2") or reveal coiled shapes of one or more CNTs (Figure 6, "3"). Consistent with the SFM, after 5 min of melt mixing, none of the MWCNTs corresponds to Figure 6, "1". This was also true for many other TEM micrographs. Thus, the localization of MWCNTs coincides with the proposed mechanism.

For CB, two notable features of the localization behavior can be seen. First, also CB is transferred from SAN into PC. Second, and despite the fact that both CB and MWCNTs experience a thermodynamic driving force toward the PC phase, the amount of CB at the blend interface is much higher than that of MWCNTs. Therefore, the high degree of interfacial coverage by CB is achieved by the enforced transfer of all particles through the blend interface during melt mixing and their higher interfacial stability and thus slower transfer speed.

4.3. Simultaneous Addition of Blend and Nanofiller Components. Accordingly, PC/SAN blends prepared by one-step blending with CB and MWCNTs reveal a significantly lower particle concentration at the blend interface (Figure 9). There, the fillers do not necessarily have to be transferred through the blend interface in order to localize within the preferred PC phase, although SAN is the earlier softening polymer in the blend.

4.4. Classification of Different Nanoscaled Fillers. Summarizing, important aspects of the localization behavior of CB and MWCNTs but also of other nanofillers can be explained with the SFM. The particle aspect ratio was identified as an important parameter for the interfacial stability and the speed of nanofiller transfer through a blend interface during melt mixing. Considering also the dispersion-state dependence of the aspect ratio, nanofillers can be subdivided in different groups according to the SFM (Table 1). Beyond CNTs, broad particle aspect ratio distributions during melt processing are obtained also for other nanofillers such as carbon nanofibres (CNF) and halloysites. Generally, the dispersion-state dependence increases with increasing aspect ratio of the individual nanoparticles and is thus low for fillers like carbon black.

Layered silicates, graphite, or MMT represent a special case, as even their exfoliated sheets are only nanoscaled in one dimension. This means that even though their aspect ratio between the in-plane dimensions and thickness is high necessarily significant parts of the layer's edges will be oriented parallel to the blend interface during transfer. Thus, intermediate interfacial stability can be derived from the SFM. The specific ability to cover significant parts of the interface with only few nanometer thick sheets enables to effectively protect two opposing blend polymers from each other. Thus, exfoliated sheets can still reveal high interfacial stability specifically for highly incompatible blend phases. Examples for their localization at the blend interface can be found in the literature.[21,45−48]

5. SUMMARY AND CONCLUSION

The mechanisms that are responsible for the localization of nanoscaled fillers during melt mixing of multiphase blend systems are still not completely understood.[25] Fast and complete transfer of MWCNTs from SAN to PC during melt blending of PC/SAN blends was observed in a previous study[6] and initiated the search for possible explanations.

As a main innovation of this study, a correlation of the aspect ratio of nanoparticles and their localization in immiscible blends during melt mixing is proposed based on the theoretical considerations of Krasovitski and Marmur.[26] Consequences were derived and discussed for the shape dependence of the interfacial stability of nanoscaled particles during melt mixing with multiphase thermoplastic blends. A fast and effective transfer mechanism from a thermodynamically unfavorable into a more favorable blend phase is predicted for CNTs, which gains its efficiency from the high aspect ratio of the nanotubes. For them, thermodynamic stable localization at the blend interface is expected to be unlikely.

In contrast, for nano-objects with low aspect ratios like carbon black, a significantly slower transfer speed and higher stability at the blend interface is predicted. The suggested shape dependence of nanofiller localization was verified by a detailed investigation of a mixed filler system consisting of low aspect ratio carbon black and high aspect ratio carbon nanotubes. Predispersing both fillers within the thermodynamically unfavorable SAN phase and subsequent melt blending with the more favorable PC phase enabled the monitoring of the interfacial transfer mechanism. It turned out that for both fillers the individual particles followed the postulated principles. This shape-dependent localization behavior was proposed to be addressed as "Slim-Fast Mechanism" (SFM), as the transfer of a slim (high aspect ratio) particle through the blend interface is proposed to be generally faster than that of a chubby (low aspect ratio) one.

The SFM was furthermore able to explain important aspects of several previous studies concerning the localization behavior of different kinds of nanofillers in polymer blends. By means of this study, we want to encourage distinguishing between fillers with high and those with low aspect ratio when discussing the localization of nanoscaled particles during melt mixing of polymer blends.

Generally, deeper understanding of nanofiller localization in blend morphologies during melt mixing in conventional extruders will be one of the key factors on the way to new cost-effective functional polymer materials.

AUTHOR INFORMATION

Corresponding Author
*E-mail poe@ipfdd.de; Tel (0049) - (0)351/4658-395; Fax-(0049) - (0)351/4658-565.

ACKNOWLEDGMENT

This research and development project is funded by the German Federal Ministry of Education and Research (BMBF) within the Framework Concept "Research for Tomorrow's Production" (fund no. 02PU2392) and managed by the Project Management Agency Karlsruhe (PTKA). We acknowledge Evonik Degussa GmbH (Marl, Germany) for consultancy and supply of carbon black and Bayer MaterialScience AG (Leverkusen, Germany) for providing polycarbonate and the employed MWCNT grade Baytubes C150HP. We thank Axel Mensch (TU Dresden) for TEM investigations of PC/SAN blends with MWCNTs and Dr. Hartmut Komber for the NMR investigation of SAN. The help of Martin Kaufmann (IPF Dresden e.V.) in fluorescence microscopic investigations of CNT filled blends is acknowledged, although the pictures could not be presented here. Furthermore, we thank Uta Reuter for preparation of ultrathin cuts and Dr. Petr Formanek (IPF Dresden e.V.) for the TEM and EFTEM investigations on the mixed filler systems.

REFERENCES

(1) Sumita, M.; Sakata, K.; Asai, S.; Miyasaka, K.; Nakagawa, H. *Polym. Bull.* **1991**, *25* (2), 265–271.
(2) Gubbels, F.; Blacher, S.; Vanlathem, E.; Jerome, R.; Deltour, R.; Brouers, F.; Teyssie, P. *Macromolecules* **1995**, *28* (5), 1559–1566.
(3) Baudouin, A.-C.; Devaux, J.; Bailly, C. *Polymer* **2010**, *51* (6), 1341–1354.
(4) Baudouin, A.-C.; Bailly, C.; Devaux, J. *Polym. Degrad. Stab.* **2010**, *95* (3), 389–398.
(5) Laredo, E.; Grimau, M.; Bello, A.; Wu, D. F.; Zhang, Y. S.; Lin, D. P. *Biomacromolecules* **2010**, *11* (5), 1339–1347.
(6) Göldel, A.; Kasaliwal, G.; Pötschke, P. *Macromol. Rapid Commun.* **2009**, *30* (6), 423–429.
(7) Pötschke, P.; Pegel, S.; Claes, M.; Bonduel, D. *Macromol. Rapid Commun.* **2008**, *29* (3), 244–251.
(8) Wu, M.; Shaw, L. L. *J. Power Sources* **2004**, *136* (1), 37–44.
(9) Wu, D. F.; Zhang, Y. S.; Zhang, M.; Yu, W. *Biomacromolecules* **2009**, *10* (2), 417–424.
(10) Li, Y.; Shimizu, H. *Macromolecules* **2008**, *41* (14), 5339–5344.
(11) Meincke, O.; Kaempfer, D.; Weickmann, H.; Friedrich, C.; Vathauer, M.; Warth, H. *Polymer* **2004**, *45* (3), 739–748.
(12) Pötschke, P.; Bhattacharyya, A. R.; Janke, A. *Polymer* **2003**, *44* (26), 8061–8069.
(13) Zou, H.; Wang, K.; Zhang, Q.; Fu, Q. *Polymer* **2006**, *47* (22), 7821–7826.
(14) Zhang, L. Y.; Wan, C. Y.; Zhang, Y. *Compos. Sci. Technol.* **2009**, *69* (13), 2212–2217.
(15) Feng, J. Y.; Chan, C. M.; Li, J. X. *Polym. Eng. Sci.* **2003**, *43* (5), 1058–1063.
(16) Persson, A. L.; Bertilsson, H. *Polymer* **1998**, *39* (23), 5633–5642.
(17) Ibarra-Gomez, R.; Marquez, A.; Valle, L.; Rodriguez-Fernandez, O. S. *Rubber Chem. Technol.* **2003**, *76* (4), 969–978.
(18) Young, T. *Philos. Trans. R. Soc. London* **1805**, *95*, 65–87.
(19) Elias, L.; Fenouillot, F.; Majeste, J. C.; Cassagnau, P. *Polymer* **2007**, *48* (20), 6029–6040.
(20) Elias, L.; Fenouillot, F.; Majeste, J. C.; Martin, G.; Cassagnau, P. *J. Polym. Sci., Part B: Polym. Phys.* **2008**, *46* (18), 1976–1983.
(21) Tong, W.; Huang, Y. J.; Liu, C. L.; Chen, X. L.; Yang, Q.; Li, G. X. *Colloid and Polymer Science* **2011**, *288* (7), 753–760.
(22) Katada, A.; Buys, Y. F.; Tominaga, Y.; Asai, S.; Sumita, M. *Colloid Polym. Sci.* **2005**, *284* (2), 134–141.
(23) Yao, S.; Zhao-Xia, G.; Jian, Y. *Macromol. Mater. Eng.* **2010**, *295* (3), 263–268.
(24) Zhang, L. Y.; Wan, C. Y.; Zhang, Y. *Polym. Eng. Sci.* **2009**, *49* (10), 1909–1917.
(25) Fenouillot, F.; Cassagnau, P.; Majeste, J. C. *Polymer* **2009**, *50* (6), 1333–1350.
(26) Krasovitski, B.; Marmur, A. *J. Adhes.* **2005**, *81* (7−8), 869–880.
(27) Baytubes C150HP Datasheet. In 2007-05-14 ed.; Bayer MaterialScience AG, Germany, 2007.
(28) Krause, B.; Boldt, R.; Pötschke, P. *Carbon* **2011**, *49* (4), 1243–1247.
(29) Callaghan, T. A.; Takakuwa, K.; Paul, D. R.; Padwa, A. R. *Polymer* **1993**, *34* (18), 3796–3808.
(30) Mamunya, Y. *Macromol. Symp.* **2001**, *170*, 257–264.
(31) Barber, A. H.; Cohen, S. R.; Wagner, H. D. *Phys. Rev. Lett.* **2004**, *92*, 18.
(32) Menzel, R.; Lee, A.; Bismarck, A.; Shaffer, M. S. P. *Langmuir* **2009**, *25* (14), 8340–8348.
(33) Stöckelhuber, K. W.; Das, A.; Jurk, R.; Heinrich, G. *Polymer* **2010**, *51* (9), 1954–1963.
(34) Nuriel, S.; Liu, L.; Barber, A. H.; Wagner, H. D. *Chem. Phys. Lett.* **2005**, *404* (4−6), 263–266.
(35) Hong, Y. C.; Shin, D. H.; Cho, S. C.; Uhm, H. S. *Chem. Phys. Lett.* **2006**, *427* (4−6), 390–393.
(36) Calberg, C.; Blacher, S.; Gubbels, F.; Brouers, F.; Deltour, R.; Jerome, R. *J. Phys. D: Appl. Phys.* **1999**, *32* (13), 1517–1525.
(37) Tchoudakov, R.; Breuer, O.; Narkis, M.; Siegmann, A. *Polym. Eng. Sci.* **1996**, *36* (10), 1336–1346.
(38) Thongruang, W.; Balik, C. M.; Spontak, R. J. *J. Polym. Sci., Part B: Polym. Phys.* **2002**, *40* (10), 1013–1025.
(39) Zaikin, A. E.; Karimov, R. R.; Arkhireev, V. P. *Colloid J.* **2001**, *63* (1), 53–59.
(40) Xu, Z. B.; Zhao, C.; Gu, A. J.; Fang, Z. P.; Tong, L. F. *J. Appl. Polym. Sci.* **2007**, *106* (3), 2008–2017.
(41) Cheah, K.; Forsyth, M.; Simon, G. P. *J. Polym. Sci., Part B: Polym. Phys.* **2000**, *38* (23), 3106–3119.
(42) Soares, B. G.; Gubbels, F.; Jerome, R.; Teyssie, P.; Vanlathem, E.; Deltour, R. *Polym. Bull.* **1995**, *35* (1−2), 223–228.
(43) Gubbels, F.; Jerome, R.; Teyssie, P.; Vanlathem, E.; Deltour, R.; Calderone, A.; Parente, V.; Bredas, J. L. *Macromolecules* **1994**, *27* (7), 1972–1974.
(44) Al-Saleh, M. H.; Sundararaj, U. *Composites, Part A* **2008**, *39* (2), 284–293.
(45) Pötschke, P.; Kretzschmar, B.; Janke, A. *Compos. Sci. Technol.* **2007**, *67* (5), 855–860.
(46) Hong, J. S.; Namkung, H.; Ahn, K. H.; Lee, S. J.; Kim, C. *Polymer* **2006**, *47* (11), 3967–3975.
(47) Si, M.; Araki, T.; Ade, H.; Kilcoyne, A. L. D.; Fisher, R.; Sokolov, J. C.; Rafailovich, M. H. *Macromolecules* **2006**, *39* (14), 4793–4801.
(48) Das, A.; Mahaling, R. N.; Stöckelhuber, K. W.; Heinrich, G. *Compos. Sci. Technol.* **2011**, *71* (3), 276–281.